Journal of Hazardous Materials Advances 18 (2025) 100726

Contents lists available at ScienceDirect

Journal of Hazardous Materials Advances

journal homepage: www.elsevier.com/locate/hazadv

Characterization of a low-density polyethylene-oxidizing enzyme in *Pseudomonas aeruginosa* via transcriptomic and proteomic analysis

Hong Rae Kim [a,1], Ye Eun Lee [b,1], Eunkyo Lee [b], Dong-Eun Suh [a], Donggeon Choi [a], Sukkyoo Lee [b,*]

[a] Department of Research and Development, Repla Inc., Suwon 16679, Republic of Korea
[b] Department of Brain Sciences, Graduate School, Daegu Gyeongbuk Institute of Science and Technology (DGIST), Daegu 42988, Republic of Korea

ARTICLE INFO

Keywords:
Low-density polyethylene
Biodegradation
Enzymes
Oxidation
Pseudomonas aeruginosa

ABSTRACT

Plastics have become indispensable in modern industries; however, their resistance to natural degradation poses environmental challenges. Biological degradation technologies employing microorganisms offer promising solutions. Here, we analyzed the transcriptome and proteome of *Pseudomonas aeruginosa*, a plastic-degrading microorganism found in the gut of superworms, to identify the genes and enzymes upregulated during low-density polyethylene (LDPE) degradation. Functional analyses of these upregulated genes and enzymes using the Kyoto Encyclopedia of Genes and Genomes and Gene Ontology databases revealed an increase in lipid and hydrophobic amino acid metabolism, suggesting their involvement in LDPE degradation. Based on these analyses, we identified phenylalanine monooxygenase (PAH), which is capable of oxidizing plastics. To investigate the involvement of the enzyme in LDPE degradation, *phhA* was transformed into *Escherichia coli*, and the enzymes were produced and purified. The purified enzymes were then reacted with LDPE and analyzed. The results revealed the formation of hydroxyl (-OH) and C—O groups on the LDPE surface after treatment with PAH, confirming its ability to oxidize LDPE. LDPE is highly hydrophobic and exhibits extremely low reactivity, making it resistant to degradation. The PAH introduces oxygen-containing functional groups into LDPE, increasing its reactivity and thereby facilitating its biodegradation. In this study, we discovered an enzyme capable of catalyzing the oxidation step (the initial stage of LDPE biodegradation) and experimentally validated its activity.

1. Introduction

Plastics are widely used in various industries because of their light weight, durability, and affordability. Despite the annual production of approximately 380 million tons of plastic, the recycling rate is approximately 9 % (Geyer et al., 2017). Consequently, plastics introduced into the soil and oceans undergo degradation, leading to microplastic pollution (MacLeod et al., 2021). Polyethylene accounts for 36 % of the overall plastic composition and contributes significantly to plastic pollution (Ali et al., 2021).

Biological degradation of plastics has attracted growing interest. This process is performed at room temperature and pressure, making it environmentally friendly. Recent studies have highlighted the ability of microorganisms to degrade plastic (Kim et al., 2020; Yang et al., 2014). However, the efficiency of microbial degradation in addressing plastic pollution remains relatively low.

The degradation of polyethylene is challenging because of its exclusive composition of carbon and hydrogen, necessitating the involvement of multiple enzymes for effective degradation (Singh et al., 2021). Initially, oxidoreductases act on polyethylene, initiating the formation of oxygen-containing functional groups. Subsequently, depolymerizing enzymes come into play in the second step, resulting in a reduction in molecular weight (Ghatge et al., 2020). Microbial oxidases, such as alkane monooxygenase and cytochrome P450, are involved in initial oxidation (Yeom et al., 2022; Yun et al., 2023; Jeon and Kim, 2015). Esterases, such as lipases, are presumed to be involved in the depolymerization process. Unlike polyester plastics such as polyethylene terephthalate, polyethylene consists of C—C bonds, posing a challenge for depolymerization by enzyme (Ghatge et al., 2020; Yeom et al., 2022). Therefore, the role of oxygenases in introducing oxygen into the chemically reduced material, polyethylene, to enhance its reactivity is essential.

* Corresponding author at: Department of Brain Sciences, Daegu Gyeonbuk Institute of Science and Technology, Daegu 42988, Republic of Korea.
E-mail address: slee2012@dgist.ac.kr (S. Lee).
[1] Hong Rae Kim and Ye Eun Lee contributed equally to this paper.

https://doi.org/10.1016/j.hazadv.2025.100726
Received 12 March 2025; Received in revised form 10 April 2025; Accepted 19 April 2025
Available online 19 April 2025

Table 1
Colony-forming unit of *P. aeruginosa* cultured with LDPE as the carbon source.

Time (days)	D0	D1	D2	D3
CFU/mL	4.93×10^5	3.77×10^6	1.83×10^7	3.65×10^7
Time (days)	D4	D5	D6	D7
CFU/mL	5.27×10^7	5.03×10^7	7.17×10^7	6.67×10^7

To enhance the effectiveness of plastic degradation, a comprehensive understanding of the mechanisms underlying plastic degradation and identification of pertinent enzymes are essential. Enhancing plastic degradation efficiency involves the discovery and optimization of enzymes involved in the process (Tournier et al., 2023). Recent studies have employed proteomic analysis to unravel microbial polyethylene metabolic pathways and their correlations with lipid metabolism (Zadjelovic et al., 2022; Gravouil et al., 2017). However, exploration of plastic-degrading enzymes using multiomics techniques, along with subsequent molecular biology approaches for expression and functional analyses, remains relatively limited.

In this study, we investigated *P. aeruginosa*, which is known for its capacity to degrade LDPE, with three main objectives: 1) to conduct a comprehensive analysis of the transcriptomics and proteomics of *P. aeruginosa* to identify candidate genes involved in plastic degradation.; 2) to produce and purify proteins from the selected genes using gene cloning; and 3) to assess the plastic degradation ability of the enzyme at the molecular level. Through these steps, we aimed to uncover the enzymes associated with LDPE oxidation which is the first step of degradation.

2. Materials and methods

2.1. LDPE degradation by P. aeruginosa

2.1.1. Cultivation of P. aeruginosa using LDPE as the carbon source

P. aeruginosa was cultivated using LDPE as the carbon source. *P. aeruginosa* was inoculated into LB medium and cultured for 24 h in a shaking incubator (28 °C, 130 rpm). After centrifuging 1 mL of the culture (13,000 rpm, 5 min), a cell pellet was obtained. The pellet was resuspended in 1 mL of liquid carbon-free basal medium (LCFBM) and subjected to additional centrifugation to eliminate residual nutrients. This washing procedure was repeated thrice. Subsequently, cells were cultured in 25 mL of LCFBM containing 0.4 g of LDPE (weight-average molecular weight [M_w] ~4000 and number-average molecular weight [M_n] ~1700, Sigma-Aldrich, MO) as the exclusive carbon source. Inoculation was performed at a 1/100 dilution based on an OD of 1.0. After a 7-day incubation period, the LDPE degradation capability of *P. aeruginosa* was assessed.

2.1.2. Colony-forming units (CFU) counting

To verify microbial proliferation using LDPE as the carbon source, CFU were quantified. One milliliter of culture sample was combined with 9 mL of LCFBM. Following six consecutive dilutions of this solution, 100 μL was spread on LB agar plates and incubated for 24 h. CFU/mL was calculated by counting the number of colonies in the diluted solutions.

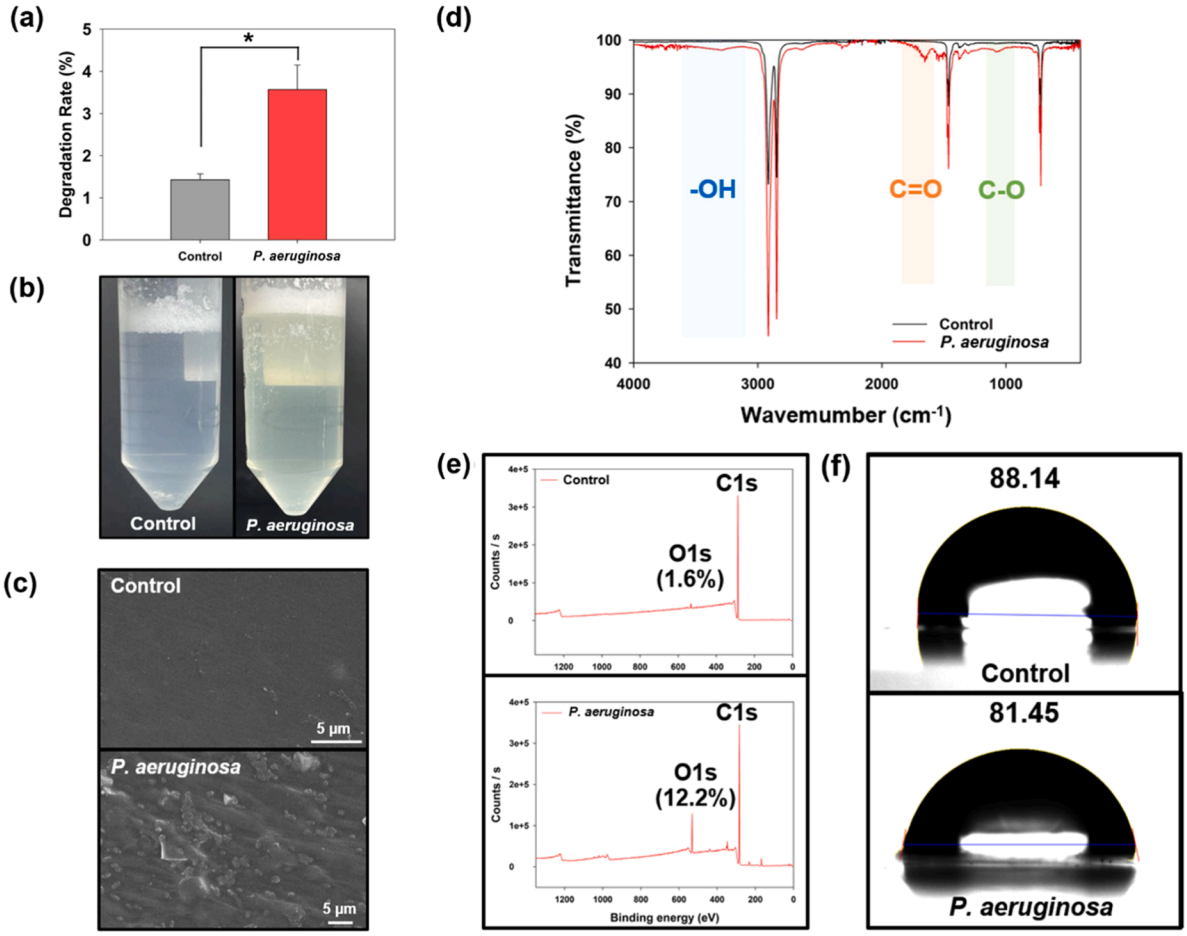

Fig. 1. LDPE-degrading bacteria, *P. aeruginosa.* (a) LDPE degradation rate over 7 days by *P. aeruginosa*. (b) *P. aeruginosa* proliferation using LDPE as the carbon source. (c) SEM image showing surface erosion of LDPE by *P. aeruginosa*. (d) Analysis of chemical groups on LDPE surfaces using FT-IR. (e) Elemental analysis of the LDPE surface using XPS. (f) Contact angle measurement on the LDPE surface.

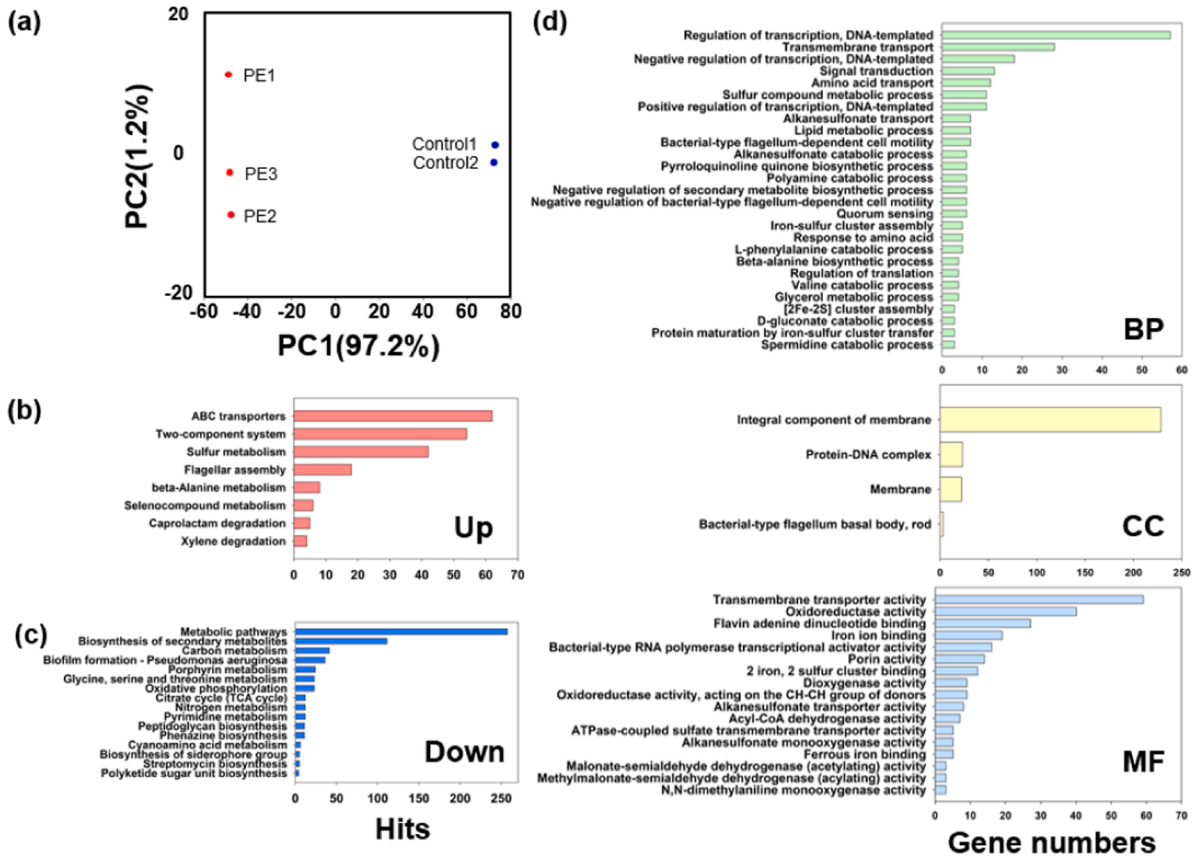

Fig. 2. Transcriptome analysis of *P. aeruginosa* cultured with LDPE as the carbon source. (a) Changes in gene expression patterns of *P. aeruginosa* observed through PCA plot. (b) Pathways associated with upregulated genes analyzed using the KEGG database. (c) Pathways associated with downregulated genes analyzed using the KEGG database. (d) Biological processes, cellular components, and molecular functions associated with upregulated genes analyzed using the GO database.

2.1.3. *Weight-loss measurement*

The dry weights of the plastics were measured to evaluate LDPE biodegradation. After cultivation, the plastics were collected using a cell strainer (pore size: 40 μm, SPL, Korea) and subjected to an overnight treatment with 2 % SDS to eliminate microorganisms adhered to the plastic surface. Subsequently, the plastics were thoroughly washed twice with deionized (DI) water and oven-dried at 60 °C for 24 h.

2.1.4. *SEM imaging*

To conduct SEM imaging and FT-IR, XPS, and contact angle analyses, plastic films are required. The LDPE films (density: 0.93 g/cm^3) were cut into 2 × 2 cm pieces. Subsequently, the films were subjected to the cultivation method outlined in Section 2.1.1. The surface characteristics of the LDPE films were examined using field-emission SEM (Merlin Compact, Zeiss, Germany). The films were securely affixed with carbon tape and coated with platinum, and SEM images were captured. Biofilm formation and corrosion of the film surface were evaluated using SEM to assess the biodegradation capabilities of the candidate plastic degraders.

2.1.5. *ATR FT-IR spectroscopy*

The LDPE film was subjected to a 24-hour treatment with 2 % SDS and washed with DI water to eliminate the biofilm. To assess the changes in the chemical structures of the LDPE films, an ATR FT-IR spectrometer (iS50, Thermo Fisher Scientific, MA, USA) was used to examine alterations in functional groups. The FT-IR analysis employed single-bounce attenuated total reflection spectroscopy, covering wavenumbers from 400 to 4000 cm^{-1}.

2.1.6. *X-ray photoelectron spectroscopy*

X-ray photoelectron spectroscopy (XPS, K-Alpha, Thermo Electron, MA,) was used to analyze the elements and binding energies on the surface of the LDPE film. The samples were secured with carbon tape and subjected to measurements in the energy range of 276–300 eV for the C1s scan and 0–1350 eV for the survey scan.

2.1.7. *Contact angle analysis*

Contact angle analysis was conducted to assess changes in surface hydrophilicity resulting from LDPE degradation. The film samples were prepared by fixing both edges of the LDPE films to a glass slide with cellophane tape. Approximately 15 μL of water was then applied to the surface using a contact angle analyzer (Phoenix 300, SEO, Suwon, Korea). Measurements were taken at three different locations, and the average values were calculated.

2.2. *Transcriptomic analysis of P. aeruginosa during LDPE degradation*

2.2.1. *mRNA sequencing*

To unravel the alterations in the transcriptome during LDPE biodegradation, *P. aeruginosa* was cultured in minimal media with LDPE as the carbon source for 7 days, and subsequently, RNA sequencing was performed. The control group consisted of *P. aeruginosa* cultured in LB for the same duration of 7 days. Total RNA concentration was calculated using Quant-IT RiboGreen (Invitrogen, CA) and the integrity of the total RNA was assessed. Only high-quality RNA (RIN>7.0) was used for library construction. Libraries were prepared with 1 μg of total RNA using the Illumina TruSeq Stranded mRNA Sample Prep Kit (Illumina Inc., CA). Bacterial rRNA-depleted samples were generated using the NEB-Next rRNA Depletion Kit (NEB, MA,) and a cDNA library was constructed. The cDNA library was quantified using KAPA Library Quantification kits (KAPA BIOSYSTEMS, MA) and qualified using

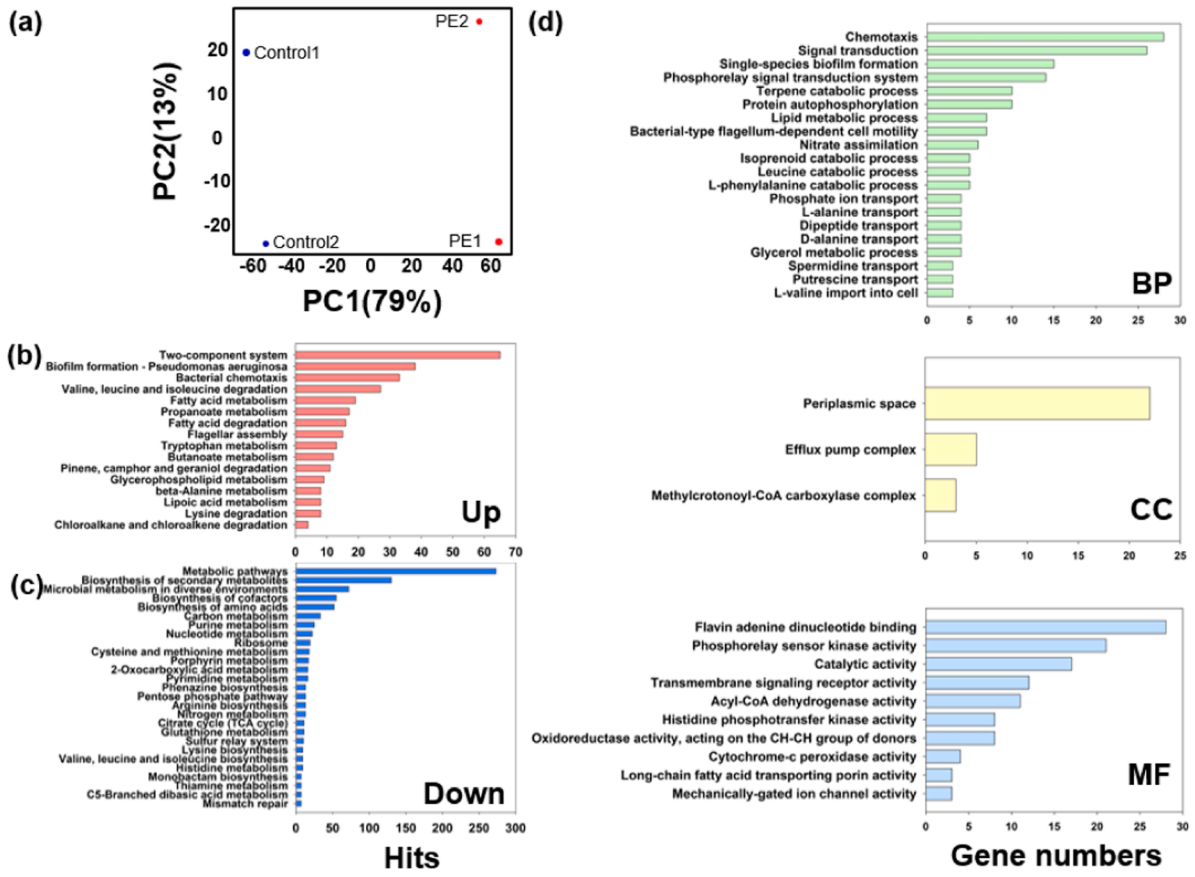

Fig. 3. Proteome analysis of *P. aeruginosa* cultured with LDPE as the carbon source. (a) Changes in protein expression patterns of *P. aeruginosa* observed through PCA plot. (b) Pathways associated with upregulated proteins analyzed using the KEGG database. (c) Pathways associated with downregulated proteins analyzed using the KEGG database. (d) Biological processes, cellular components, and molecular functions associated with upregulated proteins analyzed using the GO database.

TapeStation D1000 ScreenTape (Agilent Technologies, CA). Indexed libraries were subjected to paired-end (2 × 100 bp) sequencing using an Illumina NovaSeq system (Illumina Inc.) by Macrogen Inc. (Seoul, Korea).

2.2.2. *mRNA-Seq data analysis*

Raw reads were processed to remove low-quality and adapter sequences using Trimmomatic 0.38. The reads were aligned to *P. aeruginosa* PAO1 using Bowtie 1.1.2 (Langmead et al., 2009). The reference genome sequence of *P. aeruginosa* PAO1 (GCF_000006765.1) and annotation data were downloaded from NCBI (https://www.ncbi.nlm.nih.gov/assembly/GCF_000006765.1/). Aligned reads were assembled and the relative abundance of genes was estimated using HTSeq v0.10.0 (Anders et al., 2015). Statistical analysis was performed to identify differentially expressed genes (DEGs) using the estimated abundance of each gene in the samples. Genes with one more than zeroed Read Count values in the samples were excluded. The filtered data were log2-transformed and subjected to TMM normalization. Statistical significance of the differential expression data was determined using exactTest (EdgeR) and fold change (p-value<0.05, $|\log2FC| \geq 1$). Functional annotation of DEGs was performed using DAVID (https://david.ncifcrf.gov/home.jsp) against public databases such as the Kyoto Encyclopedia of Genes and Genomes (KEGG) and Gene Ontology (GO). PCA was used to visualize the similarities among the samples.

2.3. *Proteomic analysis of P. aeruginosa during LDPE degradation*

2.3.1. *Sample preparation for proteomics*

To examine alterations in the proteome during LDPE biodegradation, *P. aeruginosa* was cultured in minimal media with LDPE as the carbon source for 7 days, followed by LC-MS analysis. As a control group, *P. aeruginosa* cultured for the same duration of 7 days in LCFBM supplemented with 2 % glucose was used to mitigate potential interference from extraneous proteins in the proteome data caused by LB medium.

Bacterial samples were suspended in lysis buffer (8 M urea, 0.1 M Tris–HCl buffer, pH 8.5) containing a protease inhibitor cocktail (Roche Diagnostics, Basel, Switzerland) and sonicated. The protein concentration was quantified using the Pierce BCA Protein Assay Kit (Thermo Fisher Scientific). The filter-aided sample preparation method on a Microcon 30 K centrifugal filter device (Millipore, MA,) was used for protein digestion. Reduction with Tris(2-carboxyethyl)phosphine and alkylation with iodoacetic acid were followed by trypsin digestion. The resulting peptides were desalted and eluted on C18 spin columns.

2.3.2. *LC-MS/MS proteomic analysis*

The samples were analyzed using an UltiMate 3000 RSLC nano LC system (Thermo Fisher Scientific) coupled with a Q Exactive Plus mass spectrometer (Thermo Scientific). The peptides were loaded onto an Acclaim PepMap 100 Trap Column (Thermo Fisher Scientific) and subsequent peptide separation was performed using an Acclaim PepMap RSLC analytical column (Thermo Fisher Scientific). Mass spectra were acquired in the data-dependent mode with an automatic switch between full scan (m/z 400–2000) and 10 data-dependent MS/MS scans.

MS/MS raw files of each analysis were searched using Proteome Discoverer™ software (ver. 2.5) against *P. aeruginosa* database downloaded from UniProt. MS/MS data were analyzed using peptide-spectrum match validation step and SEQUEST HT process. After the searching process, data with FDR below 0.01 and at least six peptides in length were selected. Functional annotation of differentially expressed

Table 2
Functional analysis of the genes and proteins upregulated during LDPE degradation.

Function		KEGG	GO
Transmembrane transport	Transcriptome	ABC transporter, Two-component system	Integral component of membrane, Transmembrane transporter activity, Porin activity
	Proteome	Two-component system	Long-chain fatty acid transporting, porin activity
Lipid metabolism	Transcriptome	Lipid metabolic process	Acyl-CoA dehydrogenase activity
	Proteome	Fatty acid degradation, Lipoic acid metabolism	Lipid metabolic process, Acyl-CoA dehydrogenase activity
Amino acid metabolism	Transcriptome	Beta-Alanine metabolism	Polyamide catabolic process, amino acid catabolic process (L-phenylalanine, Valine)
	Proteome	Amino acid degradation (Valine, Leucine, Isoleucine, Lysine)	Amino acid metabolism (L-phenylalanine, Leucine, l-alanine, d-alanine, l-valine), Nitrate assimilation
Oxidoreductase activity	Transcriptome	Sulfur metabolism	Iron-sulfur cluster assembly, Oxidoreductase activity (acting on the CH—CH group of donors), Dioxygenase activity, Monooxygenase activity
	Proteome	-	Oxidoreductase activity (acting on the CH-CH group of donors), Cytochrome-c peroxidase activity

proteins was performed using DAVID (https://david.ncifcrf.gov/home.jsp) against public databases such as the KEGG and GO. PCA was used to visualize the similarities among the samples.

2.4. Expression and purification of cloned gene, phhA

2.4.1. Cloning of phenylalanine monooxygenase gene

PCR was conducted using primers targeting *phhA*, which encodes PAH in the genomic DNA of *P. aeruginosa* (Table S1). The gDNA served as the template for the first-round amplification, which included approximately ±100 bp regions of the genes using phhA_F1, R1 primers. Subsequently, the PCR product from the first round was used as a template for the second round of PCR, employing phhA_F2, R2 to amplify the gene sequences. The PCR conditions included initial denaturation at 95 °C for 10 min, denaturation at 95 °C for 45 s, annealing at 47 °C for 30 s, extension at 72 °C for 1 min, and a final extension at 72 °C for 5 min. Amplified *phhA* was purified and ligated into a pGEM-T-easy vector (Promega, WI, USA). The vector containing *phhA* gene was digested with *Not*I and *Nde*I and ligated into the pET-28b(+) vector (Sigma-Aldrich). The resulting plasmids were then transformed into *Escherichia coli* DH5α cells, extracted and sequenced. The pET-28b(+) vector containing *phhA* gene was transformed into *E. coli* BL21(DE3) cells for protein purification.

2.4.2. Expression and purification of PAH

Recombinant *E. coli* BL21(DE3) cells were cultured on LB medium containing kanamycin at 37 °C until reaching an OD600 of 0.6–0.8. Upon reaching the desired optical density, IPTG was added at a final concentration of 1 mM and the culture was further incubated for 6 h. The IPTG-induced bacterial culture was centrifuged (3000 rpm, 10 min) and the cell pellet was resuspended in 40 mL binding buffer. Sonication was performed for 25 min using an ultrasonic homogenizer and the cell lysates were centrifuged (9000 rpm, 30 min). Purification of PAH was conducted according to the Ni Sepharose FF Agarose (Cat.LT22871, LifeTein, NJ) protocol (Table S2). The flow rate was controlled at 1 mL/min and the column was filled with 5 mL His Ni Superflow resin (Code. Z5660N, Takara, Tokyo, Japan). A filter was inserted on top of the resin, and 15 mL of ddH_2O was added to wash the column. Subsequently, 15 mL binding buffer, cell lysate, another 15 mL binding buffer, followed by 40 mM washing buffer, and 60 mM washing buffer were added sequentially. Finally, 10 mL of elution buffer was added, and 1 mL fractions were collected for SDS-PAGE analysis.

Proteins were analyzed following the protocol provided by the OneGel PAGE kit Plus (Biosolution, Seoul, Korea). A mixture of 40 μL of protein solution and 10 μL of 5× reductase buffer (containing SDS and DTT) was heated to 100 °C for denaturation. Next, 50 μL of the protein sample and 10 μL of Precision Plus Protein Dual Color standards marker (10–250 kDa, Bio-Rad, CA, USA) were loaded onto the gel, which consisted of 12 % acrylamide stacking and separating gels. After electrophoresis, the gels were stained with Coomassie Brilliant Blue R-250. Subsequently, the gels were fixed in a solution of 50 % methanol and 10 % glacial acetic acid, stained, destained using a solution of 40 % methanol and 10 % glacial acetic acid, and stored in 5 % glacial acetic acid solution. Contaminants, including imidazole, were removed via dialysis against 1× PBS (pH 7) by changing the buffer three times using high-retention seamless cellulose tubing (Sigma-Aldrich). The concentration of purified PAH was determined using the Bradford assay.

2.5. Functional analysis of PAH in LDPE oxidation

The LDPE film (ET31-FM-000151, Goodfellow, UK, M_w~240,000 Da) were treated with enzymes at a concentration of 0.5 g/L, using 50 mM sodium phosphate buffer (pH 5, 6, 7) at 30 °C for 30 days.

2.5.1. Chemical analysis of LDPE oxidation by enzyme

The LDPE film was treated with PAH in a glass vial containing 50 mM sodium phosphate buffer for 30 days. The LDPE film was subjected to a 4-hour treatment with 2 % SDS and washed with deionized water to remove the residual enzyme attached to the film. The LDPE film was subjected to FT-IR analysis to assess the chemical modifications induced by PAH. The potassium bromide pellet method was employed as follows: The LDPE film was dissolved in a solvent mixture containing 1,2,4-Trichlorobenzene and 0.015 % butylated hydroxytoluene, and the solution was maintained in a glass vial at 160 °C for 10 min to achieve a final concentration of 2 mg/mL. Subsequently, the solvent was evaporated under nitrogen gas for 6 h. The LDPE film pellets were compressed at room temperature under a pressure of 6 MPa for 1 min using a 13 mm diameter pellet die and digital hydraulic presser (CrushIR, Pike Technologies, WI, USA). Pellets were created by blending 1–2 mg of each sample with 100 mg of potassium bromide. The analyses were performed using an FT-IR spectrometer (Thermo Fisher Scientific) in the transmission mode. Scans were conducted in the range of 4000 to 500 cm^{-1}. The changes in the elemental composition of the plastic surface were examined by measuring the binding energy using X-ray photoelectron spectroscopy (Thermo Scientific). The samples were secured with carbon tape and subjected to measurements in the energy range 276–300 eV for the C1s scan. Thermogravimetric (TGA) analysis was performed to assess the thermal stability of oxidized LDPE. Approximately 10 mg of the sample was heated from 50 to 600 °C at a rate of 10 °C/min. The analysis was conducted under nitrogen at a flow rate of 60 mL/min using a TGA analyzer (TA Instruments, DE, USA).

2.5.2. Evaluation of alkane hydroxylase activity of PAH

Alkane hydroxylase activity of purified PAH was measured by a

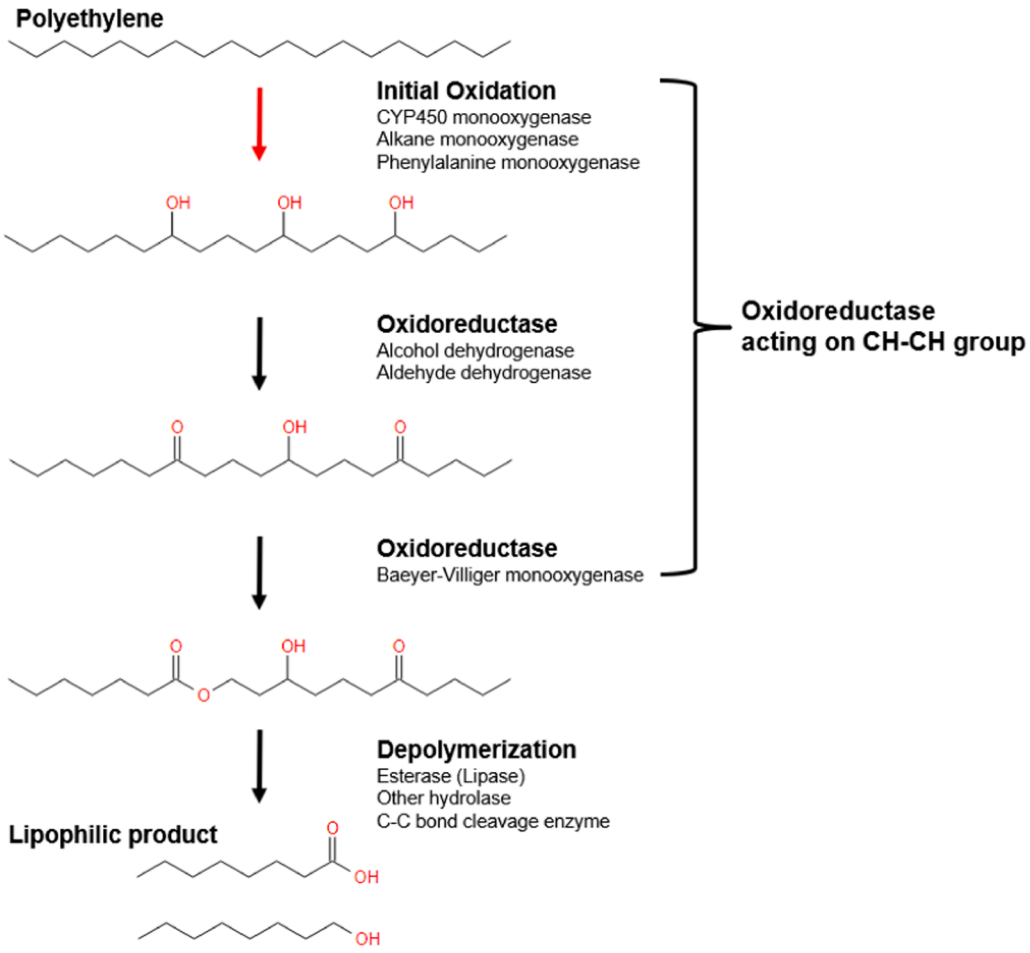

Fig. 4. Putative LDPE degradation pathway and key enzymes based on transcriptome and proteome analyses.

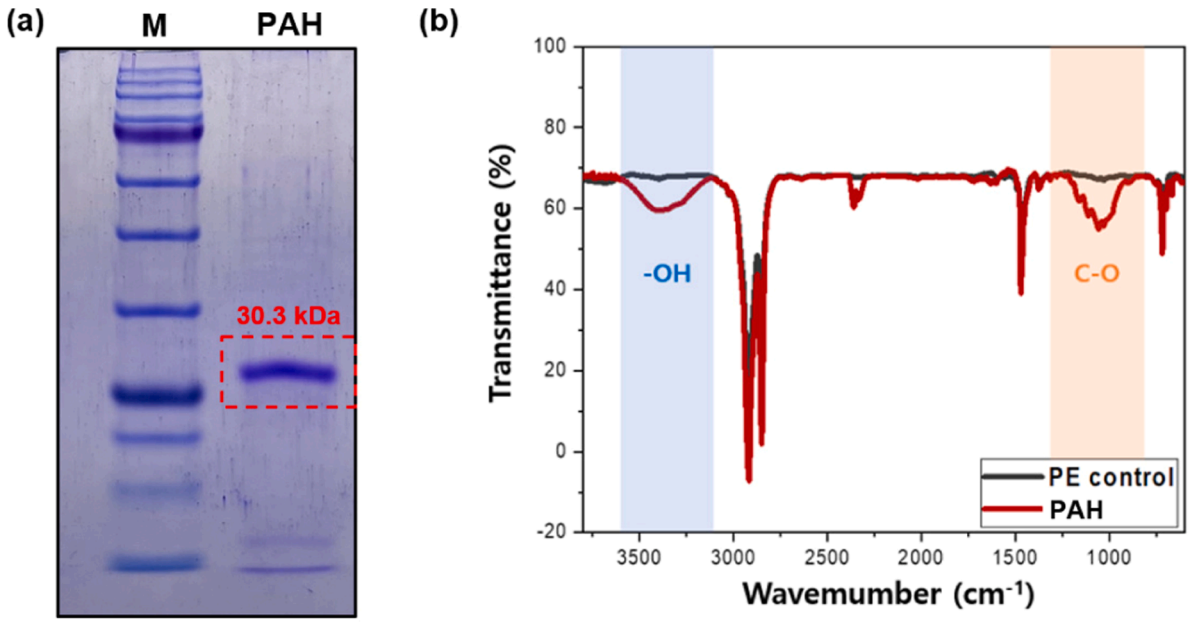

Fig. 5. FT-IR analysis of LDPE surface treated with PAH. (a) Purification of PAH (b) Analysis of chemical functional groups using FT-IR for PAH-treated LDPE.

continuous method with slight modification (Das and Negi, 2024). The reaction mixture for the enzyme assay contained 50 mM sodium phosphate buffer (pH 5.0), 2 mM NADH, 0.05 μg of enzyme, and n-dodecane (1 mM, 2 mM, or 5 mM) in a total volume of 1 mL. Enzyme activity was tested by absorbance at 340 nm in UV–Vis spectrophotometer (SpectraMax 384 plus, Molecular Devices, CA, USA) (Mishra and Singh,

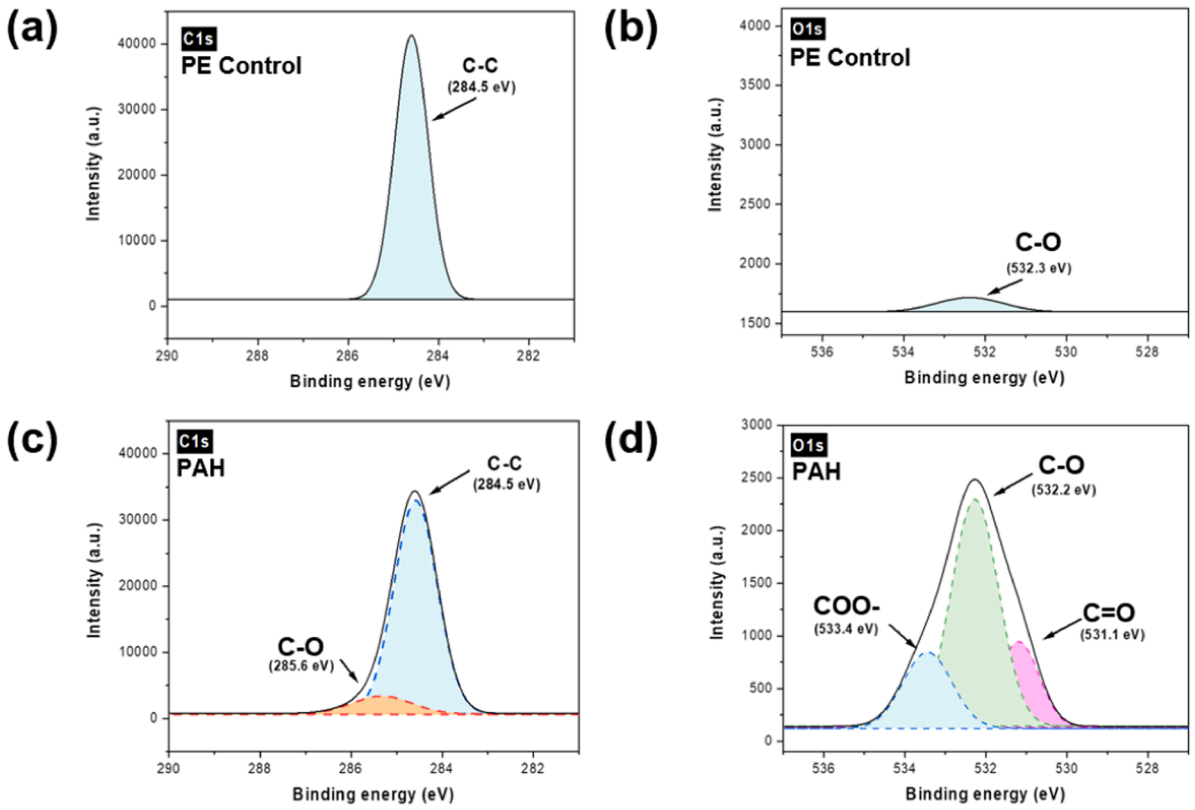

Fig. 6. XPS analysis of LDPE surface treated with PAH. Analysis of binding energy using XPS for (a) C1s and (b) O1s binding energy of the LDPE control sample. (c) C1s and (d) O1s binding energy of the PAH-treated sample.

Table 3
Enzyme kinetics analysis of PAH.

	K_m (M)	V_{max} (μM/min, Unit)	Unit/mg
Alkane Hydroxylation	1.97×10^{-3}	0.751	1.50×10^{4}

2012). The rate of NADH consumption was determined by monitoring the change in absorbance at 340 nm at room temperature for 15 min. V_{max} and K_m values were calculated using the Michaelis-Menten and Lineweaver-Burk equations.

2.5.3. Analysis of LDPE molecular weight by enzyme

The number-average molecular weight (M_n), weight-average molecular weight (M_w) and z-average molecular weight (M_z) of LDPE were determined using high-temperature gel permeation chromatography (HT-GPC). After a 30-day incubation with PAH, the LDPE film was dissolved in a mixed solvent of TCB and 0.04 % BHT to a concentration of 1.5 mg/mL, and the mixture was filtered through a 0.26 μm stainless steel mesh. The mixtures (300 μL) were injected into a HT-GPC operating at an eluent flow rate of 1.0 mL/min and a temperature of 160 °C (EcoSEC HLC-8421 GPC/HT, Tosoh Bioscience, Tokyo, Japan). The potential degradation products from depolymerization were analyzed using GC–MS (Text S1).

2.6. Structural analysis of LDPE oxidizing enzyme, PAH

To analyze the structural characteristics of PAH, we utilized the structure model of *P. aeruginosa* PAH (AF_AFP43334F1) available in the Protein Data Bank. To investigate interactions with LDPE, docking simulations were conducted using alkane compounds with structural similarity to LDPE. The docking simulations were performed using CB-Dock2, a tool for ligand–protein binding prediction (Liu et al., 2022). The protein structure was visualized based on hydrophobicity. As ligands, we used a series of alkanes: hexane (C_6H_{14}), decane ($C_{10}H_{22}$), tetradecane ($C_{14}H_{30}$), octadecane ($C_{18}H_{38}$), and tetracosane ($C_{24}H_{50}$).

3. Results and discussion

3.1. LDPE degrading bacteria, P. aeruginosa

P. aeruginosa is widely recognized for its remarkable ability to degrade plastic (Lee et al., 2020). *P. aeruginosa* proliferated using LDPE as the sole carbon source in minimal medium. The initially inoculated *P. aeruginosa*, at a concentration of 4.93×10^5 CFU/mL, underwent a 100-fold increase, reaching 5.27×10^7 CFU/mL by Day 4. On Day 7, the cell count reached saturation (Table 1). Subsequently, transcriptome and proteome analyses were conducted after cultivating *P. aeruginosa* for one week. As *P. aeruginosa* proliferated, the culture medium became turbid, and 2.14 % of the LDPE was degraded over the course of 7 days (Fig. 1a and b). SEM imaging was conducted to inspect the LDPE film surface, revealing a smooth surface in the control sample, whereas the *P. aeruginosa*-cultivated sample exhibited surface corrosion (Fig. 1b).

The degradation of LDPE by *P. aeruginosa* was chemically validated through FT-IR measurements. Culturing *P. aeruginosa* resulted in the detection of peaks corresponding to -OH (3200–3600 cm^{-1}), $C = O$ (1700 cm^{-1}), and C—O (1050 cm^{-1}) in the FT-IR spectra (Fig. 1d) (Wu and Criddle, 2021). This finding was further corroborated by XPS analysis, which indicated an increase in oxygen content after *P. aeruginosa* cultivation (Fig. 1e). Contact angle analysis revealed a decrease in the contact angle (81.45°) compared with that of the control (88.14°), signifying an increase in hydrophilicity. During plastic biodegradation, plastic is oxidized, enhancing microbial biofilm formation and enzyme reactions through increased plastic hydrophilicity (Fig. 1f) (Kim et al., 2020; Yang et al., 2015). Collectively, these analyses confirmed the utilization and proliferation of *P. aeruginosa* using LDPE

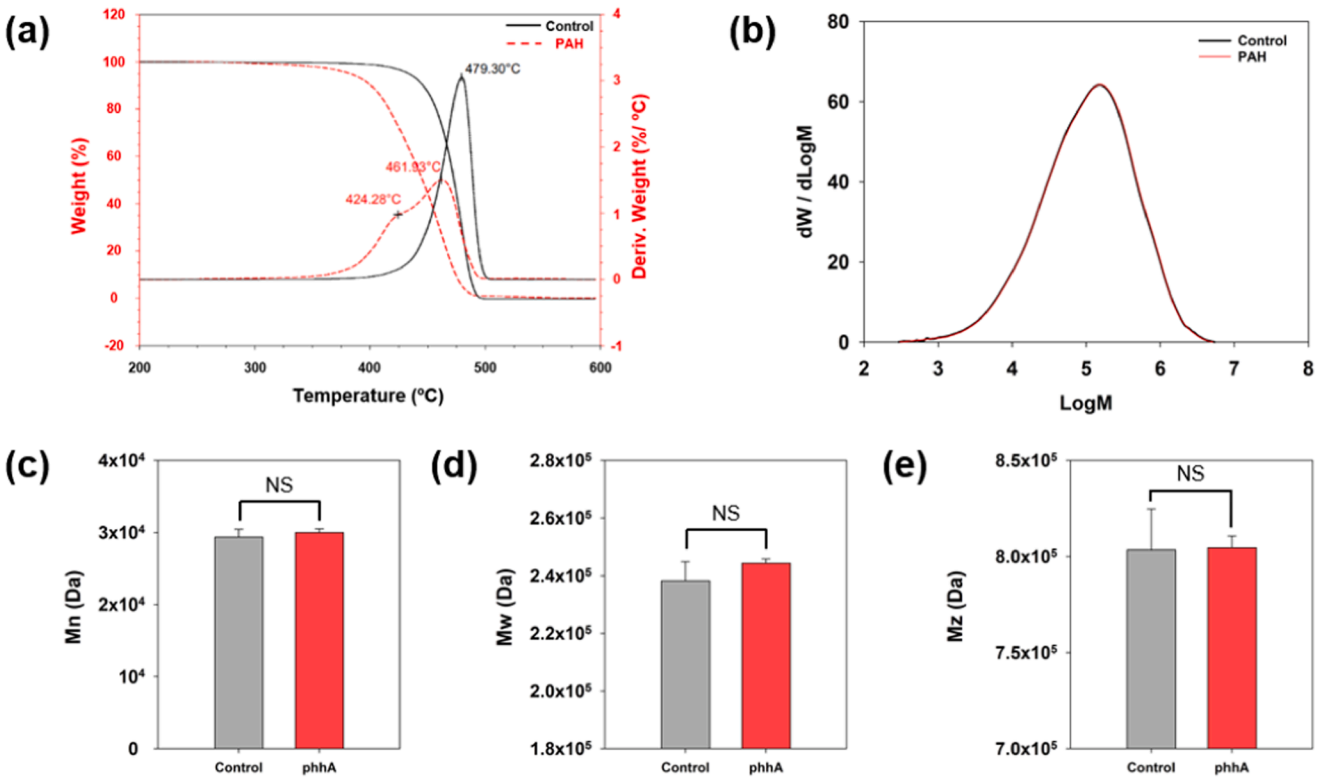

Fig. 7. Effect of PAH on the thermal stability and molecular weight of LDPE. (a) Thermal stability analysis using TGA for PAH-treated sample. (b) Overall molecular weight distribution of PAH-treated LDPE (c) Number-average molecular weight (M_n) of control, PAH samples. (d) Weight-average molecular weight (M_w) of control, PAH samples. (e) Z-average molecular weight (M_z) of control, PAH-treated samples.

Table 4
Changes in molecular weight of LDPE films treated with PAH (mean ± standard deviation, $n = 2$). M_n, number-average molecular weight M_w, weight-average molecular weight; M_z, z-average molecular weight.

Sample	M_n (Da)	M_n change (%)	M_w (Da)	M_w change (%)	M_z (Da)	M_z change (%)
Control	29,373 ± 1086	–	238,251 ± 6635	–	803,487 ± 21,274	–
PAH	29,997 ± 534	+2.1 %	244,363 ± 1458	+2.6 %	804,535 ± 6147	+0.1 %

as the carbon source.

3.2. Transcriptomic analysis of *P. aeruginosa*

Transcriptome analysis of *P. aeruginosa* cultured with LDPE as the sole carbon source revealed the upregulation of 1170 genes and downregulation of 1023 genes (Table S3). Principal component analysis distinctly clustered samples from the control and PE groups, indicating transcriptional changes associated with LDPE metabolism (Fig. 2a). To elucidate the functions of these genes, upregulated and downregulated genes were categorized by related pathway using the KEGG database and sorted based on the number of hits (Fig. 2b and c). ABC transporters may be involved in the transport of intermediate molecules generated during LDPE degradation (Borst et al., 2000). Additionally, enzymes responsible for degrading hydrophobic ring structures such as caprolactam and xylene contribute to LDPE oxidation (Kadri et al., 2017).

Subsequently, genes were categorized based on their associated biological processes using the GO database (Figs. 2d and S1). Transmembrane transport may be involved in the transport of LDPE metabolic intermediates. The lipid metabolic process was found to participate in the intracellular metabolism of depolymerized LDPE intermediates (Kong et al., 2019). Owing to the structural similarity between LDPE and lipids, LDPE enters the TCA cycle through lipid metabolic pathways within cells (Zadjelovic et al., 2022). Additionally, an amino acid catabolic process was identified, and it is noteworthy that the relevant amino acids, l-phenylalanine and valine, contained hydrophobic residues. These results suggested the potential degradation of hydrophobic LDPE intermediates through hydrophobic amino acid metabolism. Analysis of genes based on their cellular component, which represents their expression location, revealed upregulation in the membrane and downregulation in the cytoplasm. This result suggests that enhanced expression of transport proteins is required for the transportation of LDPE intermediates.

Genes were categorized based on molecular function, revealing an increase in transmembrane transporter activity, in line with KEGG and biological process analyses. Moreover, oxidoreductase activity increased, specifically involving genes acting on the CH—CH group. LDPE is a polymer composed solely of carbon and hydrogen and is directly influenced by oxidoreductases acting on the C—H groups, playing a crucial role in plastic degradation (Inderthal et al., 2021). Oxidoreductases are the enzymes involved in oxidation/reduction processes, such as oxygenases, oxidases, and dehydrogenases. Among these, the most crucial enzyme in the initial stages of plastic degradation is oxygenase, which incorporates oxygen into plastics (Liang et al., 2018). The upregulated genes include monooxygenases and dioxygenases, both of which require electron donors. Flavin adenine dinucleotide (FAD) binding signifies the activation of oxygenases that receive electrons from flavoproteins and FADH2 during plastic oxidation (Tables S4 and S5) (Morikawa, 2010). Additionally, oxygenases commonly feature iron-sulfur clusters in their active sites or rely on iron-sulfur proteins as electron donors (Britt et al., 2020). The upregulation of iron-sulfur clusters and ferrous iron binding signifies the activation of these oxygenases.

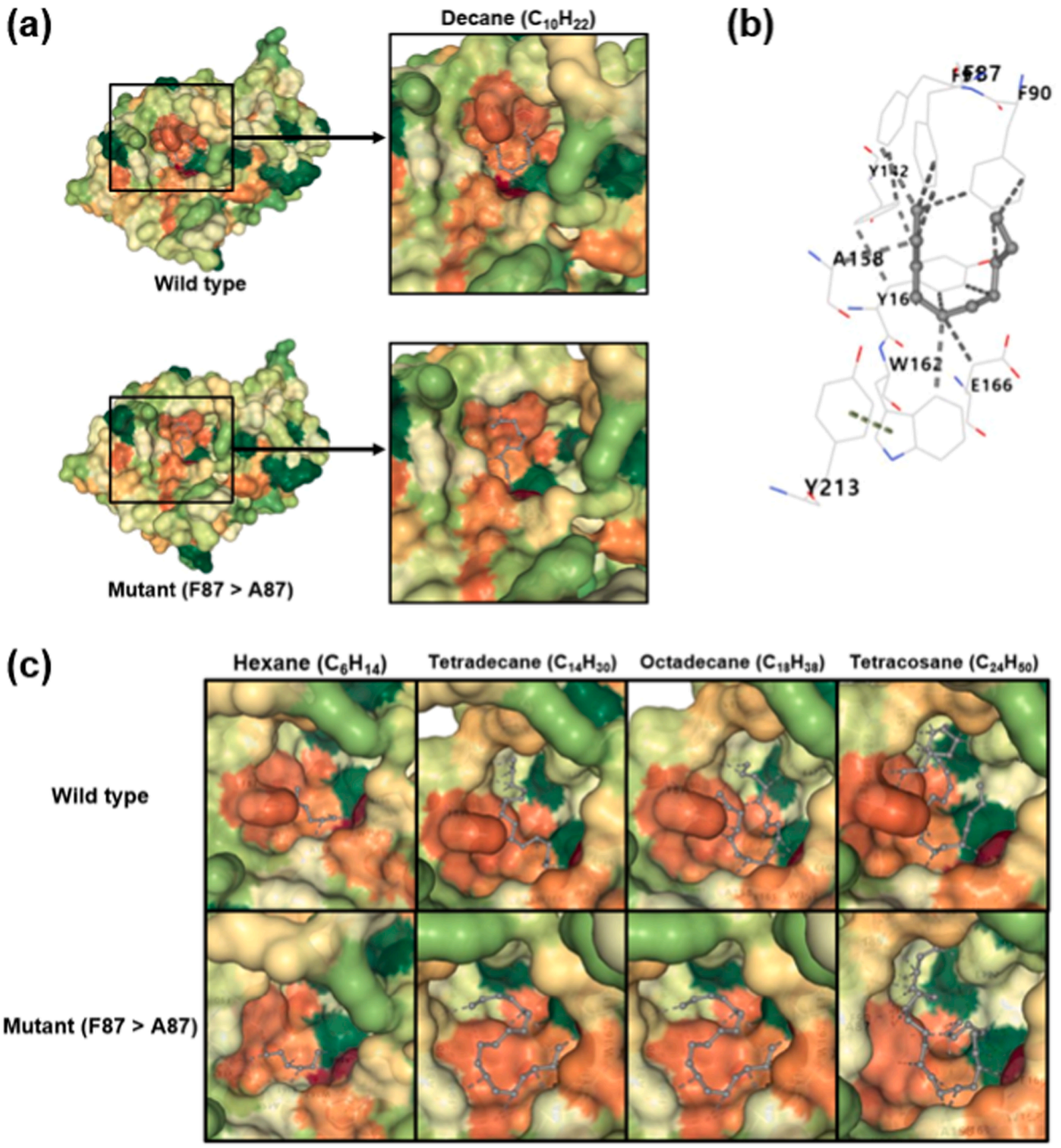

Fig. 8. Structural analysis of PAH and a proposed variant for enhanced efficiency. (a) Overall enzyme structure and the hydrophobic (red) active site. (b) Interaction between the ligand (decane) and the hydrophobic amino acid residues within the enzyme's active site. (c) Docking simulation results using a long-chain alkane molecule as the ligand for both the wild-type and mutant (F87A) enzymes.

3.3. Proteomic analysis of P. aeruginosa

Proteomic analysis of *P. aeruginosa* cultivated with LDPE as the sole carbon source revealed upregulation and downregulation of 888 and 870 proteins, respectively (Table S6). Principal component analysis demonstrated distinct clustering of samples from the control and PE groups (Fig. 3a). The overall protein analysis results closely resembled those of the transcriptome analysis. KEGG database analysis highlighted the involvement of fatty acid degradation and lipoic acid metabolism in the metabolism of LDPE intermediate molecules (Fig. 3b and c) (Zadjelovic et al., 2022; El-Sherif et al., 2022). Additionally, an increase in the degradation of hydrophobic amino acids (valine, leucine, isoleucine, alanine, and tryptophan) was observed. These results suggested the potential degradation of hydrophobic LDPE intermediates through hydrophobic amino acid metabolism.

By utilizing the GO database to categorize proteins according to biological processes, lipid metabolic and hydrophobic amino acid catabolic processes (Leucine and l-phenylalanine) were increased, corroborating the findings from the KEGG analysis (Figs. 3d and S2). Additionally, nitrate assimilation was upregulated. As LDPE comprises only carbon and hydrogen and lacks nitrogen, microorganisms can convert LDPE metabolic intermediates into amino acids via nitrogen fixation (Yang et al., 2023). Increased hydrophobic amino acid transport (L-alanine, d-alanine, and l-valine) further supports this possibility. Analysis of proteins based on cellular components revealed upregulation of proteins in the periplasmic space, with downregulation in the cytosol and cytoplasm. Long-chain fatty acid-transporting porin activity increased, suggesting its involvement in the intracellular transport of LDPE degradation intermediates (LeMoine et al., 2020). Furthermore, the upregulation of oxidoreductase activity acting on the CH—CH group

of donors indicates the expression of enzymes directly engaged in LDPE degradation. Flavin adenine dinucleotide binding suggested the potential involvement of enzymes receiving electrons from $FADH_2$ during LDPE degradation (Tischler et al., 2020).

3.4. Putative pathway for LDPE degradation mediated by P. aeruginosa

Hydrophobic amino acid and lipid metabolism emerged as commonly identified metabolic pathways in both the transcriptome and proteome analyses (Table 2). Although lipid metabolism is considered a key pathway for plastic degradation, our analysis suggested the potential degradation of hydrophobic intermediates via the hydrophobic amino acid degradation pathway (Gravouil et al., 2017). Examination of gene and protein functions revealed consistent upregulation of transporter proteins and oxidoreductase activities in the CH—CH group. Transporter proteins, such as long-chain fatty acid-transporting porins, facilitate the transport of hydrophobic intermediate molecules into cells, whereas oxidoreductases play a crucial role in plastic degradation (Zadjelovic et al., 2022; Kong et al., 2019; Tao et al., 2023).

These results suggest a putative pathway for LDPE degradation (Fig. 4). The initial step in PE degradation is oxidation by oxygenases. This step introduces hydroxyl groups (–OH) into the LDPE backbone, thereby increasing its biological reactivity. As oxidation progresses, the modified PE becomes susceptible to further enzymatic reactions. A variety of oxidoreductases—such as alcohol dehydrogenase, aldehyde dehydrogenase, and Baeyer-Villiger monooxygenase—act on CH–CH groups, leading to the formation of carbonyl groups and ester bonds. Subsequently, depolymerization-related enzymes such as esterases and C–C bond cleavage enzymes contribute to the generation of lipophilic intermediate molecules. These intermediates can be transported into the cell via lipid transport membrane proteins and utilized as energy sources through lipid metabolism and hydrophobic amino acid metabolism (Fig. S3). Based on these findings, we focused on identifying the key enzymes involved in the initial oxidative step of LDPE degradation.

3.5. Putative LDPE oxygenase: PAH

Among the 247 genes that were upregulated simultaneously in both the transcriptome and proteome, the majority were associated with transporter functions, acyl-CoA dehydrogenase (involved in lipid metabolism), and largely uncharacterized hypothetical proteins (Table S9). Oxygenases are capable of initiating the oxidation of polyolefin plastics, which are composed solely of carbon and hydrogen. In this study, only three monooxygenases were found to be simultaneously upregulated in both the transcriptome and proteome analyses: cytochrome P450, alkane monooxygenase, and PAH (Yun et al., 2023; Jeon and Kim, 2015; Kong et al., 2019). Notably, the mRNA expression level of PAH increased by 3.16-fold in microbial samples degrading LDPE, and the enzyme expression, analyzed through proteomic analysis, increased by 5.84-fold. However, the role of PAH in plastic degradation remains unclear.

PAH acts on the phenyl residue of l-phenylalanine, a hydrophobic amino acid, forming a hydroxyl group and oxidizing l-phenylalanine into l-tyrosine (Joh et al., 1986). Unlike cytochrome P450 and alkane monooxygenase, which are membrane proteins, PAH is a cytoplasmic enzyme (Barnaba et al., 2017). This characteristic renders PAH suitable for plastic degradation applications. PAH is expressed in soluble form, which enables its mass expression and purification. Therefore, this enzyme is well-suited for investigating functions and improving performance. Additionally, the ease of large-scale production of PAH makes it highly suitable for plastic degradation.

3.6. Enzymatic LDPE oxidation via PAH

3.6.1. PAH purification

The proteins produced from recombinant *phhA* in *E. coli* BL21(DE3) were purified using affinity chromatography and confirmed by SDS-PAGE (Fig. 5a). A protein of approximately 30 kDa was observed, which is consistent with the known size of PAH, indicating successful protein expression. Moreover, no other proteins were visible in the bands corresponding to each protein, confirming the successful purification.

3.6.2. LDPE oxidation by PAH

LDPE, a polymer composed of carbon and hydrogen, undergoes oxidation as the initial step in its biodegradation process. PAH can introduce a hydroxyl (-OH) group into C—H bonds. FT-IR analysis was conducted to examine the chemical functional groups on the surface of LDPE. When treated with PAH, C—O groups at 1050 cm^{-1} and hydroxyl groups (-OH) at 3000–3600 cm^{-1} were identified (Fig. 5b) (Jiang et al., 2021). Among the three pH conditions tested, PAH exhibited the highest oxidation activity at pH 5 (Fig. S4). Subsequently, the surface carbon binding energies of LDPE treated with PAH were examined using XPS (Table S10). In the control group, only C—C bonds were detected at 284.5 eV, whereas in the PAH-treated group, C—O bonds were identified at 285.6 eV, constituting 10.6 % of the total bonds (Fig. 6a and c) (Kim et al., 2020; Nyamjav et al., 2023). This finding was supported by the oxygen elemental analysis, with minimal oxygen detected in the control group (Fig. 6b). Although LDPE is composed solely of carbon and hydrogen, XPS, which is highly sensitive, can detect trace amounts of oxygen in the surrounding environment of the device. In the enzyme-treated group, significant increase in C—O bonds at 532.2, C═O bonds at 531.1, and COO- at 533.4 eV were observed, indicating the oxidation ability of PAH on LDPE (Fig. 6d) (Cheng et al., 2022). The C—O bond observed in the C1s and O1s scans was attributed to the formation of C—OH by PAH. This result was in line with the FT-IR findings, confirming the introduction of hydroxyl groups by PAH and the presence of C—O bonds in LDPE. A quantitative analysis of PAH activity was performed using a hydroxylation assay targeting alkane, the backbone structure of LDPE (Fig. S5). The enzyme kinetics of PAH were calculated using the Michaelis-Menten and Lineweaver-Burk equations, resulting in a K_m value of 1.97×10^{-3} M and a V_{max} of 0.751 μM/min (Unit), corresponding to an enzymatic activity of 1.50×10^4 Units/mg (Table 3).

Oxidation of LDPE by purified PAH was markedly more effective than that by *P. aeruginosa*, suggesting that overexpression or engineering of this enzyme could enhance LDPE degradation efficiency. To date, cytochrome P450 is the only enzyme experimentally validated to oxidize LDPE (Yun et al., 2023). In comparison to the FT-IR results of CYP450, PAH exhibited stronger C–O and –OH peaks, indicating a potentially greater capability for LDPE hydroxylation.

3.6.3. Effect of PAH on the thermal stability and molecular weight of LDPE

The thermal stability of LDPE was assessed using TGA, revealing thermal decomposition at 479.3 °C in the control group (Fig. 7a). Plastics exhibit distinct thermal decomposition temperatures, and alterations in these temperatures signify plastic degradation. Each substance has a specific pyrolysis temperature, which may change due to chemical modifications, such as the introduction of oxygen-containing groups. In the PAH-treated group, the decomposition temperature decreased, with maximum decomposition rates observed at 424.28 and 461.93 °C, indicating LDPE oxidation and formation of functional group (Peng et al., 2019). Additionally, the molecular weight of LDPE was analyzed using GPC, and no significant changes were observed in the GPC curve (Fig. 7b). Quantitative comparison of molecular weights revealed no statistically significant differences in M_n, M_w, and M_z (Table 4). This suggests that while PAH can oxidize LDPE, it does not facilitate depolymerization. GC–MS analysis also revealed that no low-molecular-weight products were formed after reacting PAH with LDPE, which aligns with the results from the HT-GPC analysis (Fig. S6). PAH enhances the reactivity of LDPE, which has low biological reactivity, by oxidizing it. Subsequently, the plastic can be converted into

low-molecular-weight substances and fully degraded through the action of redox enzymes, such as alcohol dehydrogenase, and depolymerases, such as hydrolase (Kim et al., 2023). Therefore, this study indicates that LDPE degradation is unlikely to occur via a single enzyme, underscoring the need for enzymes capable of depolymerization in future research. Based on the oxidative enzymes identified in this study, further research can focus on discovering depolymerizing enzymes for oxidized LDPE.

3.6.4. Structural analysis and simulation-based evaluation of PAH's binding potential to LDPE

To elucidate the structural characteristics of PAH involved in LDPE oxidation, we conducted a series of structural analyses. Docking simulations were performed using alkane compounds that share structural similarity with LDPE to assess potential interactions (Liu et al., 2022). When decane was used as the ligand, the simulation confirmed that the substrate binds within the enzyme's active site (Fig. 8a). Hydrophobicity-based visualization of the protein showed that the active site was predominantly hydrophobic, indicated by red coloring. This feature likely facilitates interactions with hydrophobic substrates such as LDPE (Enyoh et al., 2022). Additionally, the ligand was found to interact with hydrophobic amino acid residues located within the active site, further supporting its potential affinity for LDPE (Fig. 8b).

Structural analysis of the PAH active site revealed that the entrance is partially blocked by the side chain of phenylalanine at position 87 (Fig. S7). To enhance binding of high-molecular-weight alkane chains, such as LDPE, this residue was replaced with alanine—a smaller, yet hydrophobic amino acid—aiming to improve substrate accessibility and enzyme reactivity. The resulting F87A mutant exhibited a visibly enlarged active site entrance compared to the wild type.

To assess the enzyme's ability to accommodate alkane chains of varying lengths, docking simulations were conducted using hexane, decane, tetradecane, octadecane, and tetracosane as ligands. Longer alkanes were not tested due to computational limitations. All ligands successfully docked within the active sites of both the wild-type and F87A mutant, supporting the potential of PAH to act on LDPE-like substrates (Fig. 8c). Importantly, the mutant retained ligand-binding capacity despite the amino acid substitution, suggesting improved substrate accessibility without compromising activity. These findings provide a basis for future engineering of enzyme variants with enhanced efficiency for LDPE degradation.

4. Conclusion

We conducted transcriptome and proteome analyses of the plastic-degrading microbe *P. aeruginosa* to identify genes and enzymes with increased expression levels. Using the KEGG and GO databases, we analyzed the associated metabolic pathways and confirmed the potential involvement of lipid and hydrophobic amino acid metabolism in LDPE degradation. Subsequently, genes showing elevated expression levels in both transcriptome and proteome analyses were selected and oxygenases involved in the initial oxidation of plastics were identified. Remarkably, PAH, which was previously unrecognized in plastic degradation, was identified along with alkane monooxygenase and cytochrome P450 monooxygenase, both of which are known for their involvement in the initial oxidation of plastics. The oxidative capability of enzyme was confirmed by the formation of C—O, $C = O$, and -OH functional groups on the LDPE film after treatment with PAH. Further clarification of the enzyme's role may be achieved through overexpression or knockout studies, while its catalytic performance could be enhanced via rational design of structural mutants. Furthermore, the oxidative enzyme identified in this study provides a foundation for future research aimed at achieving the complete degradation of LDPE.

This study had limitations in qualitatively demonstrating the oxidative abilities of plastic. Hence, further research is required to develop quantitative measurement methods for oxidation rates. Additionally, Subsequent research should focus on evaluating the enzyme's activity across a range of pH and temperature conditions to identify the optimal reaction environment. Furthermore, exploring the potential industrial applications of enzymes through mass production and purification can significantly contribute to addressing plastic pollution.

CRediT authorship contribution statement

Hong Rae Kim: Writing – original draft, Visualization, Investigation, Formal analysis, Conceptualization. **Ye Eun Lee:** Visualization, Investigation, Formal analysis. **Eunkyo Lee:** Validation, Investigation. **Dong-Eun Suh:** Investigation, Funding acquisition. **Donggeon Choi:** Writing – review & editing, Investigation. **Sukkyoo Lee:** Writing – review & editing, Validation, Project administration, Methodology, Investigation, Funding acquisition, Formal analysis, Conceptualization.

Declaration of competing interest

The authors declare that they have no known competing financial interests or personal relationships that could have appeared to influence the work reported in this paper.

Acknowledgement

This study was supported by the Tech Incubator Program for Startups funded by the Ministry of Small and Medium Enterprises and Startups, Republic of Korea (no. S3136229). This work was also supported by the DGIST R&D Program of the Ministry of Science and ICT, Korea (21-BRP-04 and 22-BRP-04) and the DGIST start-up fund. We thank Jang-hee Cho for his assistance with the structural analysis of the protein.

Supplementary materials

Supplementary material associated with this article can be found, in the online version, at doi:10.1016/j.hazadv.2025.100726.

Data availability

Data will be made available on request.

References

Ali, S.S., Elsamahy, T., Al-Tohamy, R., Zhu, D., Mahmoud, Y.A., Koutra, E., Metwally, M. A., Kornaros, M., Sun, J., 2021. Plastic wastes biodegradation: mechanisms, challenges and future prospects. Sci. Total Environ. 780, 146590. https://doi.org/10.1016/j.scitotenv.2021.146590. From NLM Medline.

Anders, S., Pyl, P.T., Huber, W., 2015. HTSeq–a Python framework to work with high-throughput sequencing data. Bioinformatics 31 (2), 166–169. https://doi.org/10.1093/bioinformatics/btu638. From NLM Medline.

Barnaba, C., Gentry, K., Sumangala, N., Ramamoorthy, A., 2017. The catalytic function of cytochrome P450 is entwined with its membrane-bound nature. F1000Res (6). Austin, R. N., Born, D., Lawton, T. J., Hamilton, G. E. Protocols for purifying and characterizing integral membrane AlkB enzymes. *Hydrocarbon and Lipid Microbiology Protocols: Biochemical Methods* **2016**, 133-147.

Borst, P., Zelcer, N., van Helvoort, A., 2000. ABC transporters in lipid transport. Biochim. Biophys. Acta 1486 (1), 128–144. https://doi.org/10.1016/s1388-1981(00)00053-6. From NLM Medline.

Britt, R.D., Rao, G., Tao, L., 2020. Bioassembly of complex iron-sulfur enzymes: hydrogenases and nitrogenases. Nat. Rev. Chem. 4 (10), 542–549. From NLM PubMed-not-MEDLINE.

Cheng, Y., Chen, J., Bao, M., Li, Y., 2022. Surface modification ability of paracoccus sp. indicating its potential for polyethylene terephthalate degradation. Int. Biodeterior. Biodegrad. 173, 105454.

Das, S., Negi, S., 2024. A novel strategy for partial purification of alkane hydroxylase from P. chrysogenum SNP5 through reconstituting its native membrane into liposome. Sci. Rep. 14 (1), 3779. https://doi.org/10.1038/s41598-024-54074-0. From NLM Medline.

El-Sherif, D.M., Eloffy, M.G., Elmesery, A., Abouzid, M., Gad, M., El-Seedi, H.R., Brinkmann, M., Wang, K., Al Naggar, Y., 2022. Environmental risk, toxicity, and biodegradation of polyethylene: a review. Environ. Sci. Pollut. Res. Int. 29 (54), 81166–81182. https://doi.org/10.1007/s11356-022-23382-1. From NLM Medline.

Enyoh, C.E., Maduka, T.O., Duru, C.E., Osigwe, S.C., Ikpa, C.B., Wang, Q., 2022. In sillico binding affinity studies of microbial enzymatic degradation of plastics. J. Hazard. Mater. Adv. 6, 100076.

Geyer, R., Jambeck, J.R., Law, K.L., 2017. Production, use, and fate of all plastics ever made. Sci. Adv. 3 (7) e1700782.
Ghatge, S., Yang, Y., Ahn, J.-H., Hur, H.-G., 2020. Biodegradation of polyethylene: a brief review. Appl. Biolog. Chem. 63, 1–14.
Gravouil, K., Ferru-Clement, R., Colas, S., Helye, R., Kadri, L., Bourdeau, L., Moumen, B., Mercier, A., Ferreira, T., 2017. Transcriptomics and lipidomics of the environmental strain rhodococcus ruber point out consumption pathways and potential metabolic bottlenecks for polyethylene degradation. Environ. Sci. Technol. 51 (9), 5172–5181. https://doi.org/10.1021/acs.est.7b00846. From NLM Medline.
Inderthal, H., Tai, S.L., Harrison, S.T., 2021. Non-hydrolyzable plastics–an interdisciplinary look at plastic bio-oxidation. Trend. Biotechnol. 39 (1), 12–23.
Jeon, H.J., Kim, M.N, 2015. Functional analysis of alkane hydroxylase system derived from *Pseudomonas aeruginosa* E7 for low molecular weight polyethylene biodegradation. Int. Biodeterior. Biodegrad. 103, 141–146. Yoon, M. G., Jeon, H. J., Kim, M. N. Biodegradation of polyethylene by a soil bacterium and AlkB cloned recombinant cell. *J Bioremed Biodegrad* **2012**, *3* (4), 1-8.
Jiang, S., Su, T., Zhao, J., Wang, Z., 2021. Biodegradation of polystyrene by tenebrio molitor, galleria mellonella, and zophobas atratus larvae and comparison of their degradation effects. Polym. (Basel) 13 (20), 3539.
Joh, T.H., Hwang, O., Abate, C., 1986. Phenylalanine hydroxylase, tyrosine hydroxylase, and tryptophan hydroxylase. Neurotransmitt. Enzym. 1–32.
Kadri, T., Rouissi, T., Kaur Brar, S., Cledon, M., Sarma, S., Verma, M., 2017. Biodegradation of polycyclic aromatic hydrocarbons (PAHs) by fungal enzymes: a review. J. Environ. Sci. (China) 51, 52–74. https://doi.org/10.1016/j.jes.2016.08.023. From NLM Medline. Zhang, Z., Hou, Z., Yang, C., Ma, C., Tao, F., Xu, P. Degradation of n-alkanes and polycyclic aromatic hydrocarbons in petroleum by a newly isolated *Pseudomonas aeruginosa* DQ8. *Bioresour Technol* **2011**, *102* (5), 4111-4116. 10.1016/j.biortech.2010.12.064 From NLM Medline.
Kim, H.R., Lee, C., Shin, H., Kim, J., Jeong, M., Choi, D., 2023. Isolation of a polyethylene-degrading bacterium, Acinetobacter guillouiae, using a novel screening method based on a redox indicator. Heliyon 9 (5). https://doi.org/10.1016/j.heliyon.2023.e15731 e15731From NLM PubMed-not-MEDLINE.
Kim, H.R., Lee, H.M., Yu, H.C., Jeon, E., Lee, S., Li, J., Kim, D.H., 2020. Biodegradation of polystyrene by Pseudomonas sp. Isolated from the gut of superworms (Larvae of Zophobas atratus). Environ. Sci. Technol. 54 (11), 6987–6996. https://doi.org/10.1021/acs.est.0c01495. From NLM Medline.
Kong, H.G., Kim, H.H., Chung, J.H., Jun, J., Lee, S., Kim, H.M., Jeon, S., Park, S.G., Bhak, J., Ryu, C.M., 2019. The galleria mellonella hologenome supports microbiota-independent metabolism of long-chain hydrocarbon beeswax. Cell Rep. 26 (9), 2451–2464. https://doi.org/10.1016/j.celrep.2019.02.018 e2455From NLM Medline.
Langmead, B., Trapnell, C., Pop, M., Salzberg, S.L, 2009. Ultrafast and memory-efficient alignment of short DNA sequences to the human genome. Genom. Biol. 10 (3). https://doi.org/10.1186/gb-2009-10-3-r25. R25From NLM Medline. Li, H., Handsaker, B., Wysoker, A., Fennell, T., Ruan, J., Homer, N., Marth, G., Abecasis, G., Durbin, R., Genome Project Data Processing, S. The Sequence Alignment/Map format and SAMtools. *Bioinformatics* **2009**, *25* (16), 2078-2079. 10.1093/bioinformatics/btp352 From NLM Medline.
Lee, H.M., Kim, H.R., Jeon, E., Yu, H.C., Lee, S., Li, J., Kim, D.-H, 2020. Evaluation of the biodegradation efficiency of four various types of plastics by *Pseudomonas aeruginosa* isolated from the gut extract of superworms. Microorganisms 8 (9), 1341. Tamnou, E. B. M., Arfao, A. T., Nougang, M. E., Metsopkeng, C. S., Ewoti, O. V. N., Moungang, L. M., Nana, P. A., Takang-Etta, L.-R. A., Perrière, F., Sime-Ngando, T. Biodegradation of polyethylene by the bacterium *Pseudomonas aeruginosa* in acidic aquatic microcosm and effect of the environmental temperature. *Environmental Challenges* **2021**, *3*, 100056. Kale, S. K., Deshmukh, A. G., Dudhare, M. S., Patil, V. B. Microbial degradation of plastic: a review. *Journal of Biochemical Technology* **2015**, *6* (2), 952-961.
LeMoine, C.M., Grove, H.C., Smith, C.M., Cassone, B.J., 2020. A very hungry caterpillar: polyethylene metabolism and lipid homeostasis in larvae of the greater wax moth (Galleria mellonella). Environ. Sci. Technol. 54 (22), 14706–14715. Mishra, R., Chavda, P., Kumar, R., Pandit, R., Joshi, M., Kumar, M., Joshi, C. Exploring genetic landscape of low-density polyethylene degradation for sustainable troubleshooting of plastic pollution at landfills. *Science of The Total Environment* **2024**, *912*, 168882.
Liang, Y., Wei, J., Qiu, X., Jiao, N., 2018. Homogeneous oxygenase catalysis. Chem. Rev. 118 (10), 4912–4945. https://doi.org/10.1021/acs.chemrev.7b00193. From NLM Medline. Abbasian, F., Lockington, R., Mallavarapu, M., Naidu, R. A Comprehensive Review of Aliphatic Hydrocarbon Biodegradation by Bacteria. *Appl Biochem Biotechnol* **2015**, *176* (3), 670-699. 10.1007/s12010-015-1603-5 From NLM Medline.
Liu, Y., Yang, X., Gan, J., Chen, S., Xiao, Z.X., Cao, Y., 2022. CB-Dock2: improved protein-ligand blind docking by integrating cavity detection, docking and homologous template fitting. Nucl. Acid. Res. 50, W159–W164. https://doi.org/10.1093/nar/gkac394. W1From NLM Medline.
MacLeod, M., Arp, H.P.H., Tekman, M.B., Jahnke, A., 2021. The global threat from plastic pollution. Science 373 (6550), 61–65. https://doi.org/10.1126/science.abg5433. From NLM Medline.
Mishra, S., Singh, S., 2012. Microbial degradation of n-hexadecane in mineral salt medium as mediated by degradative enzymes. Bioresour. Technol. 111, 148–154.
Morikawa, M., 2010. Dioxygen activation responsible for oxidation of aliphatic and aromatic hydrocarbon compounds: current state and variants. Appl. Microbiol. Biotechnol. 87 (5), 1595–1603. https://doi.org/10.1007/s00253-010-2715-z. From NLM Medline.
Nyamjav, I., Jang, Y., Park, N., Lee, Y.E., Lee, S., 2023. Physicochemical and structural evidence that Bacillus cereus isolated from the gut of waxworms (Galleria mellonella larvae) biodegrades polypropylene efficiently in vitro. J. Polym. Environ. (10), 4274–4287. https://doi.org/10.1016/j.chemosphere.2023.140763. *31*Ji, S. H., Yoo, S., Park, S., Lee, M. J. Biodegradation of low-density polyethylene by plasma-activated Bacillus strain. *Chemosphere* **2024**, *349*, 140763From NLM Medline.
Peng, B.Y., Su, Y., Chen, Z., Chen, J., Zhou, X., Benbow, M.E., Criddle, C.S., Wu, W.M., Zhang, Y., 2019. Biodegradation of polystyrene by dark (Tenebrio obscurus) and yellow (Tenebrio molitor) mealworms (Coleoptera: tenebrionidae). Environ. Sci. Technol. 53 (9), 5256–5265. https://doi.org/10.1021/acs.est.8b06963. From NLM Medline.
Singh, R., Mehrotra, T., Bisaria, K., Sinha, S., 2021. Environmental hazards and biodegradation of plastic waste: challenges and future prospects. Bioremed. Environ. Sustain. 193–214.
Tao, X., Ouyang, H., Zhou, A., Wang, D., Matlock, H., Morgan, J.S., Ren, A.T., Mu, D., Pan, C., Zhu, X., et al., 2023. Polyethylene degradation by a rhodococcous strain isolated from naturally weathered plastic waste enrichment. Environ. Sci. Technol. 57 (37), 13901–13911. https://doi.org/10.1021/acs.est.3c03778. From NLM Medline.
Tischler, D., Kumpf, A., Eggerichs, D., Heine, T., 2020. Styrene monooxygenases, indole monooxygenases and related flavoproteins applied in bioremediation and biocatalysis. Enzymes 47, 399–425. https://doi.org/10.1016/bs.enz.2020.05.011. From NLM Medline. Kaur, T., Lakhawat, S. S., Kumar, V., Sharma, V., Neeraj, R. R. K., Sharma, P. K. Polyaromatic Hydrocarbon Specific Ring Hydroxylating Dioxygenases: Diversity, Structure, Function, and Protein Engineering. *Curr Protein Pept Sci* **2023**, *24* (1), 7-21. 10.2174/1389203724666221108114537From NLM Medline.
Tournier, V., Duquesne, S., Guillamot, F., Cramail, H., Taton, D., Marty, A., Andre, I., 2023. Enzymes' Power for plastics degradation. Chem. Rev. https://doi.org/10.1021/acs.chemrev.2c00644. From NLM Publisher.
Wu, W.M., Criddle, C.S., 2021. Characterization of biodegradation of plastics in insect larvae. Method. Enzymol. 648, 95–120. https://doi.org/10.1016/bs.mie.2020.12.029. From NLM Medline.
Yang, J., Yang, Y., Wu, W.M., Zhao, J., Jiang, L., 2014. Evidence of polyethylene biodegradation by bacterial strains from the guts of plastic-eating waxworms. Environ. Sci. Technol. 48 (23), 13776–13784. https://doi.org/10.1021/es504038a. From NLM Medline.
Yang, Y., Hu, L., Li, X., Wang, J., Jin, G., 2023. Nitrogen fixation and diazotrophic community in plastic-eating mealworms Tenebrio molitor L. Microb. Ecol. 85 (1), 264–276. https://doi.org/10.1007/s00248-021-01930-5. From NLM Medline. Ding, M. Q., Yang, S. S., Ding, J., Zhang, Z. R., Zhao, Y. L., Dai, W., Sun, H. J., Zhao, L., Xing, D., Ren, N., et al. Gut Microbiome Associating with Carbon and Nitrogen Metabolism during Biodegradation of Polyethene in Tenebrio larvae with Crop Residues as Co-Diets. *Environ Sci Technol* **2023**, *57* (8), 3031-3041. 10.1021/acs.est.2c05009 From NLM Medline.
Yang, Y., Yang, J., Wu, W.M., Zhao, J., Song, Y., Gao, L., Yang, R., Jiang, L., 2015. Biodegradation and mineralization of polystyrene by plastic-eating mealworms: part 2. Role of gut microorganisms. Environ. Sci. Technol. 49 (20), 12087–12093. https://doi.org/10.1021/acs.est.5b02663. From NLM Medline.
Yeom, S.J., Le, T.K., Yun, C.H., 2022. P450-driven plastic-degrading synthetic bacteria. Trend. Biotechnol. 40 (2), 166–179. https://doi.org/10.1016/j.tibtech.2021.06.003. From NLM Medline.
Yun, S.-D., Lee, C.O., Kim, H.-W., An, S.J., Kim, S., Seo, M.-J., Park, C., Yun, C.-H., Chi, W.S., Yeom, S.-J., 2023. Exploring a new biocatalyst from Bacillus thuringiensis JNU01 for polyethylene biodegradation. Environ. Sci. Technol. Lett 10 (6), 485–492.
Zadjelovic, V., Erni-Cassola, G., Obrador-Viel, T., Lester, D., Eley, Y., Gibson, M.I., Dorador, C., Golyshin, P.N., Black, S., Wellington, E.M.H., et al., 2022. A mechanistic understanding of polyethylene biodegradation by the marine bacterium Alcanivorax. J. Hazard Mater. 436, 129278. https://doi.org/10.1016/j.jhazmat.2022.129278. From NLM Medline.